points are defined in the region of the ends of the interval [0, 1] by the solution of Eq. (2.15). According to the data given in Table 1

$$x_{01} = 0.12/n,\ x_{0k} = (k-1)/n,\ k = 2, \ldots, n,\ x_{0n+1} = 1 - x_{01}.$$

For the function $\gamma(x) = \varphi(x)/\sqrt{x(1-x)}$, not bounded at both ends of the interval [0, 1], uniform convergence of function (1.6) to integral (1.1) occurs at n − 1 points. In this case the discrete vortices should be again arranged in the middle of each element, while the coordinates of the control points

$$x_{0k} = (k - 0.5 + \nu_k(0))/n,\ k = 1, \ldots, n_1,\ x_{0k} = (k + 0.5 - \nu_{n-k}(0))/n,\ k = n_1 + 1, \ldots, n-1,$$

where the coefficients $\nu_k(0)$ are found from Table 1.

LITERATURE CITED

1. M. A. Lavrent'ev, "Construction of the flow round an arc of given shape," Tr. TsAGI, No. 118 (1932).
2. S. M. Belotserkovskii, A Thin Bearing Surface in a Subsonic Flow of Gas [in Russian], Moscow (1965).
3. S. M. Belotserkovskii, B. K. Skripach, and V. G. Tabachnikov, A Wing in a Nonstationary Gas Flow [in Russian], Moscow (1971).
4. S. M. Belotserkovskii and B. K. Skripach, Aerodynamic Derivatives of an Aircraft and Wing at Subsonic Speeds [in Russian], Moscow (1975).
5. S. M. Belotserkovskii and M. I. Nisht, Detached and Nondetached Flow of an Ideal Liquid around Thin Wings [in Russian], Moscow (1978).
6. I. K. Lifanov and Ya. E. Polonskii, "Proof of the numerical method of discrete vortices for solving singular integral equations," Zh. Prikl. Mat. Mekh., 39, No. 4 (1975).
7. I. K. Lifanov, "Singular integral equations with one-dimensional and multiple Cauchy-type integrals," Dokl. Akad. Nauk SSSR, 239, No. 2 (1978).
8. V. É. Saren, "Convergence of the method of discrete vortices," Sib. Mat. Zh., 19, No. 2 (1978).
9. D. N. Gorelov and R. L. Kulyaev, "The nonlinear problem of the nonstationary flow of an incompressible liquid around a thin profile," Izv. Akad. Nauk SSSR, Mekh. Zhidk. Gaza., No. 6 (1971).

THE WAKE BEHIND THE BEARING BODY IN A VISCOUS LIQUID

O. S. Ryzhov and E. D. Terent'ev

UDC 532.516/517

1. Vortex Sheet. Suppose the bearing body (a wing of finite span) is loaded in a uniform flow of incompressible liquid. Assuming that the viscosity can be neglected, the most effective method of calculating the inductive resistance of the wing is as follows. The bearing surface and the contact interface formed behind it, and passing through which the tangential component of the velocity of vector is removed, are replaced by a system of attached and free vortices. The simplest version of the method operates in all with one connected vortex, which simulates the wing, and a pair of free vortices trailing from its ends. This system is sometimes called a horseshoe-shaped vortex, and it gives a lifting force (and circulation) that is constant over the whole area of the bearing surface, falling suddenly to zero at the ends of the wing. This scheme is, of course, only a rough approximation to the actual picture of the flow.

For a more accurate description of the flow field we must start from the fact that the lifting force changes over the length of the bearing surface, falling smoothly to zero at its end sections. The circulation also changes over the span of the wing, and from each point of its trailing edge a free vortex runs off which then moves downward with respect to the flow. This system of free vortices forms a vortex sheet. Although these representations were developed long ago [1, 2] they have not been of any value up to now [3]. In recent years to calculate the self-induced motion of vortex filaments the method of joining the external and

Moscow. Translated from Zhurnal Prikladnoi Mekhaniki i Tekhnicheskoi Fiziki, No. 5, pp. 83-91, September-October, 1980. Original article submitted February 26, 1980.

0021-8944/80/2105-0643$07.50

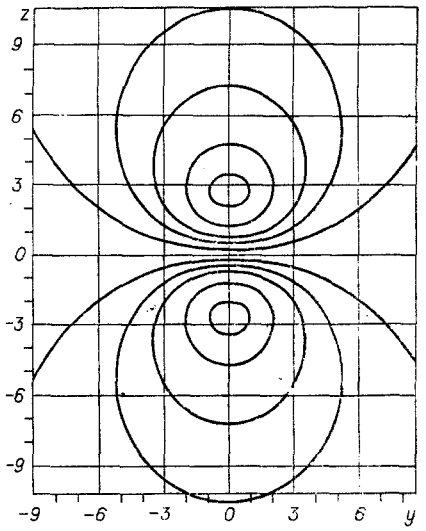

Fig. 1

internal asymptotic expansions has been used; progress in determining the field structure of wake vortices is described in [4].

The related problem is the generation, development, and decay of ring vortices. Interesting results in this area have been obtained by Lavrent'ev at the Institute of Hydrodynamics, Siberian Branch of the Academy of Sciences of the USSR, the results of which are described in [5]. The decay of vortices is discussed in [6].

Close to the wing the velocities induced by the vortices cause a displacement of the vortex filaments, and, consequently, deformation of the vortex sheet, and rolling up of the vortex sheet begins. The section of the vortex sheet transverse to the direction of the main flow enables the formation of two characteristic spirals to be detected, where a concentration of the intensity of the vortices occurs [3]. When the vortex sheet descends from the leading edges of arrow-shaped or triangular wings its intense rolling up begins immediately. The numerical method of discrete vortices recently developed enables one to obtain, using a computer, the shape of the sheet both for nonseparating flow of the leading edge of the wing and when separation from it occurs [7].

It is an extremely difficult problem to study the spirals behind the wing. The nonstationary roll-up of a semiinfinite sheet formed in the initially established plane-parallel vortex-free flow at the edge of a plane plate suddenly removed at a certain instant of time has been investigated in [8]. The solution obtained was the basis for a model of the roll-up of a vortex sheet decending from the rear edge of the wing [9]; a two-term asymptotic of the equation of the spiral was established in [10]. The theory of an ideal (nonviscous) liquid has also been used to describe the flow in the nucleus of a rolled-up sheet, which occurs at the vertex of a triangular wing [11]. To construct the velocity field induced by vortex spirals, the asymptotic method of different scales, which is based essentially on the packing density of the turns of the spiral in the region of its focus, has recently been successfully employed [12].

As is well known, the contact surfaces are blurred due to the action of the viscosity of the liquid. The viscous diffusion of the vorticity, concentrated round the turns of the spiral, when they are very close to one another in space, has been studied in [9, 13, 14]. An asymptotic analysis of the system of Navier—Stokes equations using the method of different scales leads directly to the heat-conduction equation, which satisfies the intensity of the vortex sheet as a result of an appropriate transformation of the independent variables [15].

A quite different approach was used in [16] based on the idea that the viscosity has the predominant effect on the formation of a laminar wake during the final stages of degeneration. At considerable distances from the bearing body the coils of the vortex spirals are completely broken up and disappear, although the trajectories of the particles may retain their spiral form for quite a long time. The structure of the wake in a viscous liquid can be established from the requirement that the velocity field is related to the resistance and lifting force of the wing and disappears as the values of these forces approach zero. The asymptotic

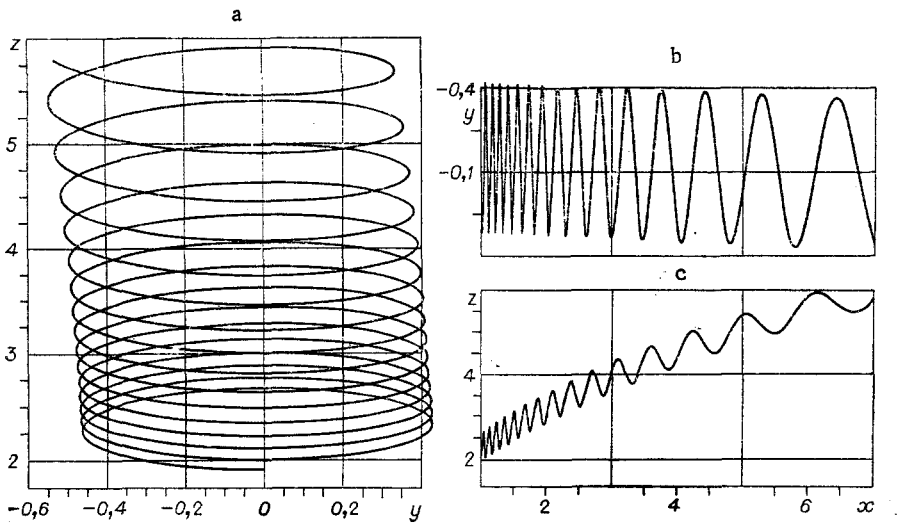

Fig. 2

solution, which describes the final stage of the propagation of a vortex trail far from the body around which the flow occurs, can be represented in the form [17]

$$v_x = -\frac{1}{4\pi x}\left(c_x + \frac{c_y}{2}\frac{y}{x}\right)\exp\left(-\frac{y^2+z^2}{4x}\right),$$
$$v_y = -\frac{c_y}{2\pi(y^2+z^2)}\left\{\frac{z^2}{2x}\exp\left(-\frac{y^2+z^2}{4x}\right) + \frac{z^2-y^2}{y^2+z^2}\left[\exp\left(-\frac{y^2+z^2}{4x}\right)-1\right]\right\}, \quad (1.1)$$
$$v_z = \frac{c_y}{\pi}\frac{yz}{y^2+z^2}\left\{\frac{1}{4x}\exp\left(-\frac{y^2+z^2}{4x}\right) + \frac{1}{y^2+z^2}\left[\exp\left(-\frac{y^2+z^2}{4x}\right)-1\right]\right\},$$

where x, y, z are the axes of a cartesian system of coordinates, and the x axis is oriented in the direction of the main uniform flow running from infinity, v_x, v_y, and v_z are the components of the vector of the disturbed velocity of the particles of gas along the axes of this system of coordinates, and c_x and c_y are constants, the values of which are proportional to the resistance coefficients and the lifting force of the wing and inversely proportional to the longitudinal scale of the wake. Both the independent variables and the components of the perturbed velocity in Eqs. (1.1) are measured in a certain dimensionless system where we take the characteristic transverse scale of the wake as the unit of length along the y and z axes, and the longitudinal scale of the wake along the x axis, and we take as the unit of velocity the velocity of the main flow.

Equations (1.1) remain true for a wake behind the body which is in a flow of compressible gas. As shown in [18], they can also be used in the transonic mode. In this case the so-called critical velocity serves as the unit of velocity and the particle density in the sonic flow is chosen as the unit of density. The specific volume of the gas, of course, varies from point to point, but relations (1.1) continue to hold since these changes come about independently. More accurately, the excess density satisfies the heat-conduction equation with a coefficient equal to the reciprocal of the Prandtl number. Only for hypersonic velocities of motion of the gas does the structure of the wake suffer qualitative changes, which are due primarily to the fact that the particles are very strongly heated, passing through the front of the head shock wave, and their entropy increases sharply [19, 20].

The role of viscosity in the motion of ring vortices has been discussed in [5], where simple mathematical models used to describe turbulent processes are also described.

2. General Properties of the Solution. We will write the equations for the current lines passing through the wake. In the system of units of measurement employed we have

$$dy/dx = \mathrm{Re}_1 v_y(x, y, z),\ dz/dx = \mathrm{Re}_1 v_z(x, y, z), \quad (2.1)$$

where the Reynolds number Re_1 is found from the above characteristic length, velocity, density, and also from the value of the first coefficient of viscosity in the unperturbed flow. The appearance of the Reynolds number on the right sides of Eqs. (2.1) is explained by the affine compression of all the distances in the wake along its longitudinal direction when changing to dimensionless variables. As regards the special small parameter ε', by means of

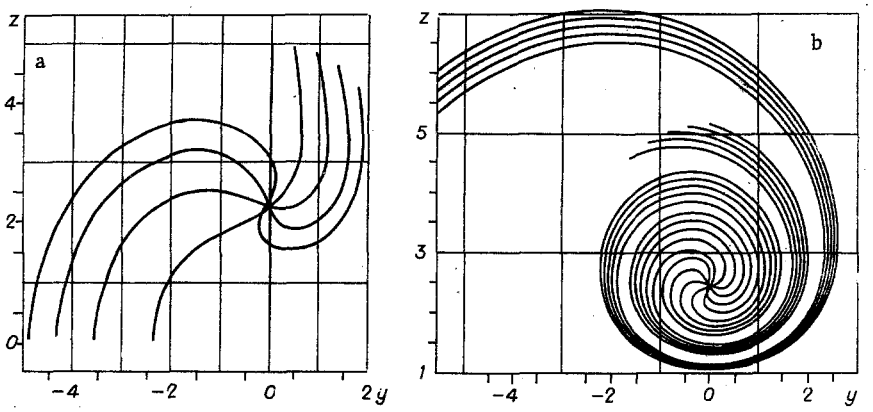

Fig. 3

which the amplitude of the perturbations was recorded in [18], we will include it in the values of the constants c_x and c_y.

Expressing the functions v_y and v_z in (2.1) by means of relations (1.1), we obtain a system of two ordinary differential equations. At points with coordinates

$$y = 0,\ 1 + z^2/2x = \exp(z^2/4x) \tag{2.2}$$

both transverse components of the vector of the perturbed velocity vanish. The solution of the last equation defines two branches $z = \pm 2.24\sqrt{x}$ of a parabola, symmetrically situated in the $y = 0$ plane. The points of intersection of these branches with the planes $x = \text{const}$ give the centers of the vortices. In order to clarify this statement we will integrate Eqs. (2.1) in the plane of the transverse cross section of the wake, fixing the coordinate $x = x_0$. The results for $x_0 = 1$ are shown in Fig. 1. The tangents to the curve shown in the figure give the field of the directions of the transverse component of the velocity vector at each point of the chosen cross section of the wake. As a whole the picture is typical for a pair of diverging and diffusing vortices. It is useful to recall that when calculating the self-induced motion of a vortex filament in an ideal (nonviscous) liquid by estimating the velocity along the axis of the vortex, according to the Biot—Savat law a logarithmic singularity is obtained if this axis is bent [1-3]. The effect of viscosity manifests itself primarily in the fact that at the center of the vortex both transverse components of the vector of the perturbed velocity disappear, but its longitudinal component remains different from zero.

We will calculate the components ω_x, ω_y, ω_z of the dimensionless vector, defining the vorticity of the flow in the wake. Retaining only the principal terms in all the formulas we have

$$\omega_x = -\frac{c_y}{8\pi}\frac{z}{x^2}\exp\left(-\frac{y^2+z^2}{4x}\right),$$
$$\omega_y = \frac{c_x}{8\pi}\frac{z}{x^2}\exp\left(-\frac{y^2+z^2}{4x}\right),\quad \omega_z = -\frac{c_x}{8\pi}\frac{y}{x^2}\exp\left(-\frac{y^2+z^2}{4x}\right). \tag{2.3}$$

Hence, the longitudinal component of the vortex vector is proportional, to a first approximation, to the lifting force of the wing, while both transverse components are proportional to its resistance. All three components have the same order of magnitude and decay with distance in accordance with the same laws. However, in practical problems of aerodynamics the lifting force of the wing considerably exceeds its resistance, in view of which the numerical value of the constant c_y will be much greater than c_x. Hence it follows that the direction of the vortex vector in the wake does not differ very much from the direction of the uniform flow from infinity.

We will obtain the position of the maxima of ω_x. By differentiating the first of Eqs. (2.3) it can be seen that the maximum values of the longitudinal component of the vortex vector occur along the branch $z = \pm 1.41\sqrt{x}$ situated in the $y = 0$ plane of the parabola. These maxima do not coincide with the centers of the vortices, but are shifted closer to the plane of symmetry of the flow $z = 0$.

3. Near Field. At first sight it would appear that the field of the directions of the transverse component of the velocity vector of the particles, which can be obtained from Fig. 1, should give a complete representation of the nature of the motion in the wake behind

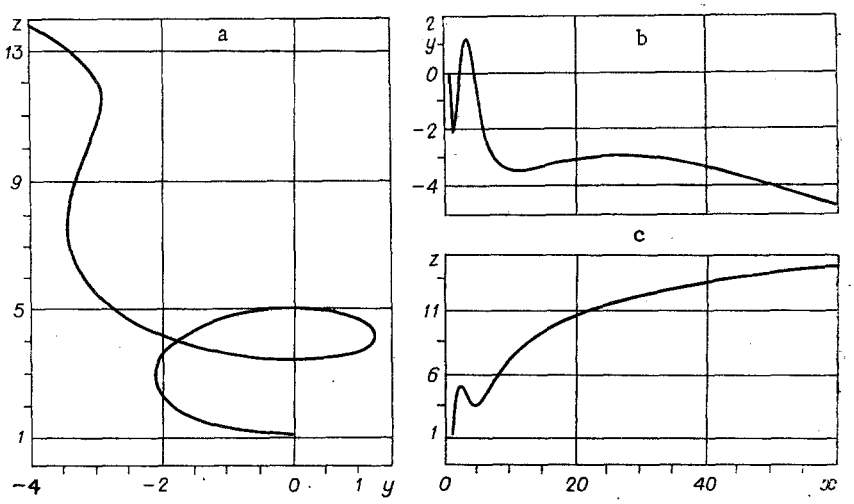

Fig. 4

the body around which the flow occurs. However, this conclusion is erroneous. As will become clear in what follows, we must distinguish between the near and far regions where the current lines differ considerably in their shape, although the overall picture shown in Fig. 1 remains unchanged when changing from one plane of transverse cross section of the wake to another.

In order to explain how the fields of motion of the gas differ in the near and far regions, we will first transform the system of equations (2.1) by introducing the new variables

$$x=\left(\frac{\mathrm{Re}_1 c_y}{2\pi}\right)^2 x_1,\quad y=\frac{\mathrm{Re}_1 c_y}{2\pi}y_1,\quad z=\frac{\mathrm{Re}_1 c_y}{2\pi}z_1. \tag{3.1}$$

In these variables the shape of the current lines is independent of the coefficients Re_1 and c_y, since

$$\frac{dy_1}{dx_1}=-\frac{1}{y_1^2+z_1^2}\left\{\frac{z_1^2}{2x_1}\exp\left(-\frac{y_1^2+z_1^2}{4x_1}\right)+\frac{z_1^2-y_1^2}{y_1^2+z_1^2}\left[\exp\left(-\frac{y_1^2+z_1^2}{4x_1}\right)-1\right]\right\},$$
$$\frac{dz_1}{dx_1}=\frac{y_1z_1}{y_1^2+z_1^2}\left\{\frac{1}{2x_1}\exp\left(-\frac{y_1^2+z_1^2}{4x_1}\right)+\frac{2}{y_1^2+z_1^2}\left[\exp\left(-\frac{y_1^2+z_1^2}{4x_1}\right)-1\right]\right\}. \tag{3.2}$$

It is determined solely by the position of the initial point when solving the system of equations (3.2). In order to see the differences in the behavior of the current lines in the near and far regions, we must either integrate the equations over a large range of variation of the indepenedent variable, or choose the initial points in different planes of transverse cross section of the wake. This sometimes makes it inconvenient to realize numerically on a computer.

In practice it turns out to be simpler to work with the system of equations (2.1) in the initial variables. By dispensing with the transformations (3.1) we can always consider the initial point situated in the $x = x_0 = 1$ plane, but it necessitates varying the coefficient $\mathrm{Re}_1 c_y/2\pi$. It can be seen that large values of this coefficient correspond to the near regions of the wake, and a reduction in its value occurs when one transfers to the far region, if the curves investigated are extended moderate distances from the initial plane $x_0 = 1$. By then reverting to transformation (3.1), we can, by fixing $\mathrm{Re}_1 c_y/2\pi$, calculate the relations obtained at different distances along the length of the wake.

The characteristic shape of the current lines for the near region is obtained for $\mathrm{Re}_1 c_y/2\pi = 1000$. Figures 2a-c show the results of the calculations when the transverse coordinates of the initial point $y_0 = 0$ and $z_0 = 1.9$. It can be seen from the projection of this curve onto the zy plane that the particles of gas execute helical motions. The axis around which the rotations occur is the trajectory of the center of one of the vortices; according to Eqs. (2.2) it is bent, receding from the plane of symmetry of the flow $z = 0$. Hence, the turns of the current line are displaced quite considerably along the span of the wing, which can be traced quite clearly from the projection on the zy plane. It can be seen

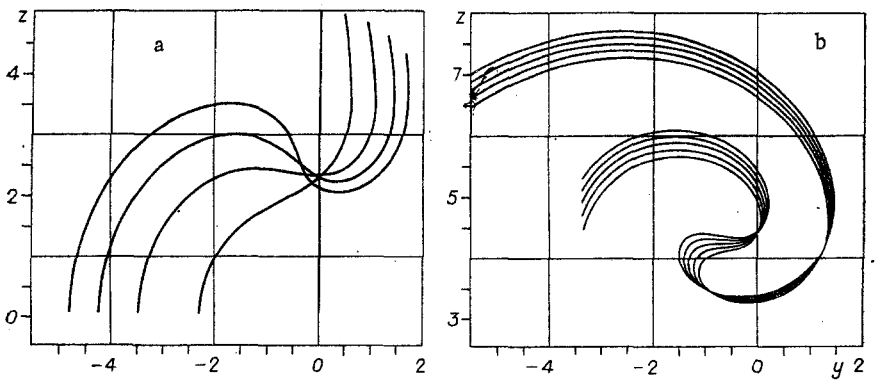

Fig. 5

from the projection on the xy plane that in addition there is a small descent of the turns in a direction opposite to the action of the lifting force of the body.

The deformation of the initial section of the straight line when its points move along current lines is even more significant. The sections of the current surfaces by the transverse planes x = const obtained in this way are shown in Fig. 3a-b. When constructing all the curves the spacing Δx between successive sections was chosen to be 0.012, but whereas in Fig. 3a the first curve shows the initial position of the section in the $x = x_0 = 1$ plane, in Fig. 3b the first curve relates to the section x = 1.192. Such a pattern will be observed experimentally if the particles are colored in some way in their initial position; this is in fact used in different methods of flow visualization [21].

Figure 3 demonstrates the spiral convolution of the current surface. This process is qualitatively similar to the convolution or a vortex sheet along its sides when either the viscosity of the liquid is completely ignored, or the effect of dissipative factors is assumed to be of the second degree [12, 15]. However, there is also a considerable difference between the spirals investigated and the vortex spirals in an ideal liquid. The development of the latter is characterized by a sawtooth distribution of the flow parameters in any direction in the x = const plane, since when passing through the contact surface in an ideal liquid the tangential component of the velocity vector suffers a discontinuity. As was shown above, in an arbitrary section of the wake, the structure of which is formed mainly due to the action of viscosity, there are always two maxima of ω_x. Although in the near region of a viscous wake the spiral form of the convolution of the current surfaces is extended, the contact surfaces are completely blurred and disappear.

4. Far Field. When Fig. 2a-c is carefully studied it is found that when the longitudinal coordinate is increased, the turns of the current line become more widely spaced. This property is by no means random, but represents the transition to the far region of the wake, where the helical form of motion of the gas particles gradually ceases. The shape of the current lines in the intermediate stage can be obtained by taking $\mathrm{Re}_1 c_y/2\pi = 100$. The results of calculations, when the initial current has transverse coordinates $y_0 = 0$ and $z_0 = 1.1$ in the $x = x_0 = 1$ plane, are shown in Fig. 4a-c. It is clear from the projection of this curve on the yz plane that the helical motion of the particles in this case reduces in all to a single rotation. Then, as the projection on the xz plane demonstrates, the current line is deflected along the wing span from the plane of symmetry of the flow z = 0 and much more slowly than the trajectory of the center of the corresponding vortex, described by the parabolic relationship (2.2). For this reason this trajectory ceases to be the axis around which the current line twists. It can be seen from the projection on the xy plane that some displacement occurs in the opposite direction to the lifting force applied to the body.

We will follow the deformation of the initial section of the straight line which is dictated by the motion of the points along the current lines. Two sections of the current surfaces by the transverse planes x = const formed in this way are shown in Fig. 5a-b. The spacing Δx between successive sections was chosen to be 0.12 each time; the first curve in Fig. 5a shows the initial position of the section in the $x = x_0 = 1$ plane, and the first curve in Fig. 5b relates to the section x = 3.76. In view of the fact that at the intermediate stage the current lines in these calculations make a single rotation around the trajectory of the center of any vortex, the spirals in Fig. 5b consist in all of a single turn.

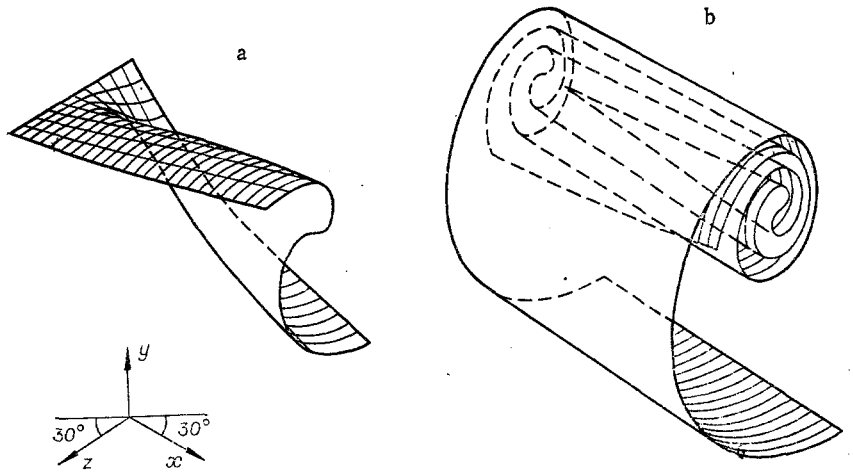

Fig. 6

When transferring into the far region of the wake itself the spiral form of the convolution of the current surfaces completely disappears. It is easy to establish the asymptotic form of the current lines here by expanding in series the exponents on the right sides of Eqs. (1.1) with the condition $y^2 + z^2 \ll x$. The correctness of the latter follows directly from the results of the calculations discussed above. As a result of simple calculations we obtain

$$\frac{dy}{dx} = -\frac{\mathrm{Re}_1 c_y}{8\pi}\frac{1}{x}, \quad \frac{dz}{dx} = -\frac{\mathrm{Re}_1 c_y}{32\pi}\frac{yz}{x^2}. \tag{4.1}$$

The system of equations (4.1) can be integrated in explicit form

$$y = -\frac{\mathrm{Re}_1 c_y}{8\pi}\ln c_1 x, \quad z = c_2 \exp\left[-\left(\frac{\mathrm{Re}_1 c_y}{16\pi}\right)^2 \frac{1+\ln c_1 x}{x}\right].$$

The main conclusion to which these relations lead is that as $x \to \infty$ the current lines suffer a vertical displacement of the order of ln x downwards (in the opposite direction to the action of the lifting force of the body), and their deflection along the wing span from the plane of symmetry of the flow z = 0 tends to a constant c_2. Numerical integration of the initial system of equations (2.1), the right sides of which are not subjected to any simplifications, leads to results in excellent agreement with the conclusion formulated if we choose $\mathrm{Re}_1 c_y/2\pi = 10$, and, as usual, places the initial point in the $x = x_0 = 1$ plane. Hence, when one moves downwards a fairly considerable distance along the flow from the bearing body, coloring [21] of the particles of gas in their initial position along a certain line should lead to visualization of the current surfaces without helical twisting. It would be interesting to verify this conclusion experimentally.

5. Current Surfaces. In order to be able to represent more clearly the process of roll-up of the current surface in the near region of the wake, it is best to return to the representation of the spatial pattern of the flow. One of the current surfaces discussed above with $\mathrm{Re}_1 c_y/2\pi = 1000$ is shown in Fig. 6a-b in a rectangular isometric projection. The longitudinal curves correspond to the position of the current lines; its limiting cross sections by the transverse planes x = const give the first and last curves in Fig. 3a-b. When the distance from the body around which the flow occurs is increased, the number of turns of the spiral twist of this surface increases gradually until the far region of the wake is reached. In agreement with the above discussion, additional roll-up of the current surfaces ceases here.

LITERATURE CITED

1. L. Prandtl and O. Titens, Hydro- and Aeromechanics [Russian translation], Vol. 2, Ob'ed. Nauch. Tekh. Izd. NKTP SSSR, Moscow–Leningrad (1935).
2. V. F. Durand (ed.), Aerodynamics [Russian translation], Vol. 2, Gos. Izd. Oboron. Promyshl., Moscow–Leningrad (1939).
3. G. K. Batchelor, Introduction to Fluid Dynamics, Cambridge Univ. Press (1967).
4. S. E. Widnall, "The structure and dynamics of vortex filaments," in: Annual Rev. Fluid. Mech., Vol. 7, Ann. Rev. Inc., Palo Alto, California (1975).

5. M. A. Lavrent'ev and B. V. Shabat, Problems of Hydrodynamics and Their Mathematical Model [in Russian], Nauka, Moscow (1973).
6. S. Leibovich, "The structure of vortex breakdwon," in: Ann. Rev. Fluid Mech., Vol. 10, Ann. Rev. Inc. Palo Alto, California (1978).
7. S. M. Belotserkovskii and M. I. Nisht, Detached and Nondetached Flow of an Ideal Fluid around a Thin Wing [in Russian], Nauka, Moscow (1978).
8. H. Kaden, "Aufwicklung einer unstabilen Unstetigkeitsfläche," Ingenieur-Archiv, Vol. 2, No. 2 (1931).
9. D. W. Moore and P. G. Saffman, "Axial flow in laminar trailing vortices," Proc. R. Soc. Ser. A, 333, No. 1545 (1973).
10. D. W. Moore, "The rolling up of a semi-infinite vortex sheet," Proc. R. Soc. Ser. A, 345, No. 1642 (1975).
11. K. W. Mangler and J. Weber, "The flow field near the centre of a rolled-up vortex sheet," J. Fluid. Mech., 30, Pt. 1 (1967).
12. J. P. Guiraud and R. Kh. Zeytounian, "A double-scale investigation of the asymptotic structure of rolled-up vortex sheets," J. Fluid Mech., 79, Pt. 1 (1977).
13. K. Kirde, "Untersuchugen über zeitliche Weiterentwicklung eines Wirbels mit vorgegebener Anfangsverteilung," Ingenieur-Archiv., 31, No. 6 (1962).
14. G. K. Batchelor, "Axial flow in trailing line vortices," J. Fluid Mech., 20, Pt. 4 (1964).
15. J. P. Guiraud and R. Kh. Zeytounian, "A note on the viscous diffusion of rolled vortex sheets," J. Fluid Mech., 90, Pt. 1 (1979).
16. S. A. Berger, Laminar Wakes, Elsevier, New York (1971).
17. L. D. Landau and E. M. Lifshits, Mechanics of Continuous Media [in Russian], GITTL, Moscow (1954).
18. O. S. Ryzhov and E. D. Terent'ev, "Perturbations connected with the production of a lifting force acting on a body in a transonic flow of a disspiating gas," Zh. Prikl. Mat. Mekh., 31, No. 6 (1967).
19. V. V. Sychev, "Flow in a laminar hypersonic wake behind a body," in: Fluid Dynamics Transactions, Vol. 3, PWN, Warsaw (1966).
20. O. S. Ryzhov and E. D. Terent'ev, "The laminar hypersonic wake behind a bearing body," Zh. Prikl. Mat. Mekh., 42, No. 2 (1978).
21. H. Werlé, "Hydrodynamic flow visualization," in: Ann. Rev. Fluid Mech., Vol. 5, Ann. Rev. Inc., Palo Alto, California (1973).

AUTOMATIC DAMPING OF VIBRATIONS OF AN AIRPLANE WING BY INTERNAL CONTROL FORCES

V. I. Merkulov

UDC 532.5

An increase in the absolute dimensions of aircraft leads to a decrease in their dynamic rigidity. Both the frequency of natural vibrations and the structural damping factor are decreased. The deformations produced by impulsive forces die down slowly, but periodic disturbances may increase as a result of resonance. All this leads to a decrease of the flying life of the structure. We study various methods of damping elastic vibrations by using internal forces. The amplitude, frequencies, and phase of the forces acting are governed by a control system. A movable mass, an internal tension, a flexible shaft, and a gyromotor are considered as a control. In contrast with the familiar method using external aerodynamic forces, an internal control continues to be effective also on the airfield where, as it turns out, the airplane is subjected to the largest dynamic load.

1. Flexural—torsional vibrations of a wing of small sweepback and large aspect ratio can be described by a two-component vector function $\{w(y, t), \theta(y, t)\}$ [1]. Here $w(y, t)$ is the vertical displacement from the equilibrium position of the elastic axis of the wing, and $\theta(y, t)$ is the rotation of a chord of the wing about the elastic axis. These quantities are functions of the coordinate y of a cross section and the time t. In terms of these variables,

Novosibirsk. Translated from Zhurnal Prikladnoi Mekhaniki i Tekhnicheskoi Fiziki, No. 5, pp. 91-99, September-October, 1980. Original article submitted March 14, 1980.

 0021-8944/80/2105-0650$07.50